



## OPEN ACCESS

## EDITED BY

Cristovao Vilela,  
University of Coimbra, Portugal

## REVIEWED BY

Ian Lawson,  
SNOLAB, Canada  
Giulia D'Imperio,  
Istituto Nazionale di Fisica Nucleare, Italy

## \*CORRESPONDENCE

KeonAh Shin,  
✉ kashin@ibs.re.kr  
HyunSu Lee,  
✉ hyunsulee@ibs.re.kr

RECEIVED 12 January 2023

ACCEPTED 04 April 2023

PUBLISHED 21 April 2023

## CITATION

Shin K, Choe J, Gileva O, Iltis A, Kim Y,  
Kim Y, Lee C, Lee E, Lee H and Lee MH  
(2023), Mass production of ultra-pure NaI  
powder for COSINE-200.  
*Front. Phys.* 11:1142849.  
doi: 10.3389/fphy.2023.1142849

## COPYRIGHT

© 2023 Shin, Choe, Gileva, Iltis, Kim, Kim,  
Lee, Lee, Lee and Lee. This is an open-  
access article distributed under the terms  
of the [Creative Commons Attribution  
License \(CC BY\)](https://creativecommons.org/licenses/by/4.0/). The use, distribution or  
reproduction in other forums is  
permitted, provided the original author(s)  
and the copyright owner(s) are credited  
and that the original publication in this  
journal is cited, in accordance with  
accepted academic practice. No use,  
distribution or reproduction is permitted  
which does not comply with these terms.

# Mass production of ultra-pure NaI powder for COSINE-200

KeonAh Shin<sup>1\*</sup>, JunSeok Choe<sup>1</sup>, Olga Gileva<sup>1</sup>, Alain Iltis<sup>2</sup>,  
Yena Kim<sup>1</sup>, Yeongduk Kim<sup>1,3</sup>, Cheolho Lee<sup>1</sup>, Eunkyung Lee<sup>1</sup>,  
HyunSu Lee<sup>1,3\*</sup> and Moo Hyun Lee<sup>1,3</sup>

<sup>1</sup>Center for Underground Physics, Institute for Basic Science (IBS), Daejeon, South Korea, <sup>2</sup>Damavan Imaging, Troyes, France, <sup>3</sup>IBS School, University of Science and Technology (UST), Daejeon, South Korea

COSINE-200 is the next phase experiment of the ongoing COSINE-100 that aims to unambiguously verify the annual modulation signals observed by the DAMA experiment and to reach the world competitive sensitivity on the low-mass dark matter search. To achieve the physics goal of the COSINE-200, the successful production of the low-background NaI(Tl) detectors is crucial and it must begin from the mass production of the ultra-low background NaI powder. A clean facility for mass-producing the pure-NaI powder has been constructed at the Center for Underground Physics (CUP) in Korea. Two years of operation determined efficient parameters of the mass purification and provided a total of 480 kg of the ultra-pure NaI powder in hand. The potassium concentration in the produced powders varied from 5.4 to 11 ppb, and the maximum production capacity of 35 kg per 2 weeks was achieved. Here, we report our operational practice with the mass purification of the NaI powder, which includes raw powder purification, recycling of the mother solution, and recovery of NaI from the residual melt after crystal growth.

## KEYWORDS

NaI powder, low-background, mass purification, recrystallization, COSINE-200

## 1 Introduction

Considerable evidence points to the existence of dark matter that could represent 27% of the Universe's total mass or energy [1–5]. One of the most promising candidates for dark matter is the Weakly Interacting Massive Particles (WIMPs), which many experimental groups have extensively searched in the last few decades [6–13]. Despite attempting to find dark matter particles in numerous experiments, only the DAMA collaboration has claimed the observation of a dark matter signal through an annual modulation signal observed in the low-energy signal region [8, 14–16]. However, there have been long-standing questions about this claim because no other experimental searches have observed similar signals [17]. Besides, possible spurious effects have been widely investigated, but none provides a convincing explanation of the modulation signal observed by DAMA/LIBRA [18, 19].

The COSINE-100 experiment has been operating at Yangyang underground laboratory in Korea with a total of 106 kg of low-background NaI(Tl) detectors during the last 6 years [6, 7, 20–24]. Although many exciting results were published, reaching an unambiguous assumption on the annual modulation signal of the DAMA experiment is far from conclusive [25, 26]. It is mainly due to the observed background rate in the COSINE-100 detectors, which is 2.5 times higher than the background of the DAMA detectors [21, 27]. To take on the challenge in the world's competitive searches for low-mass dark matter

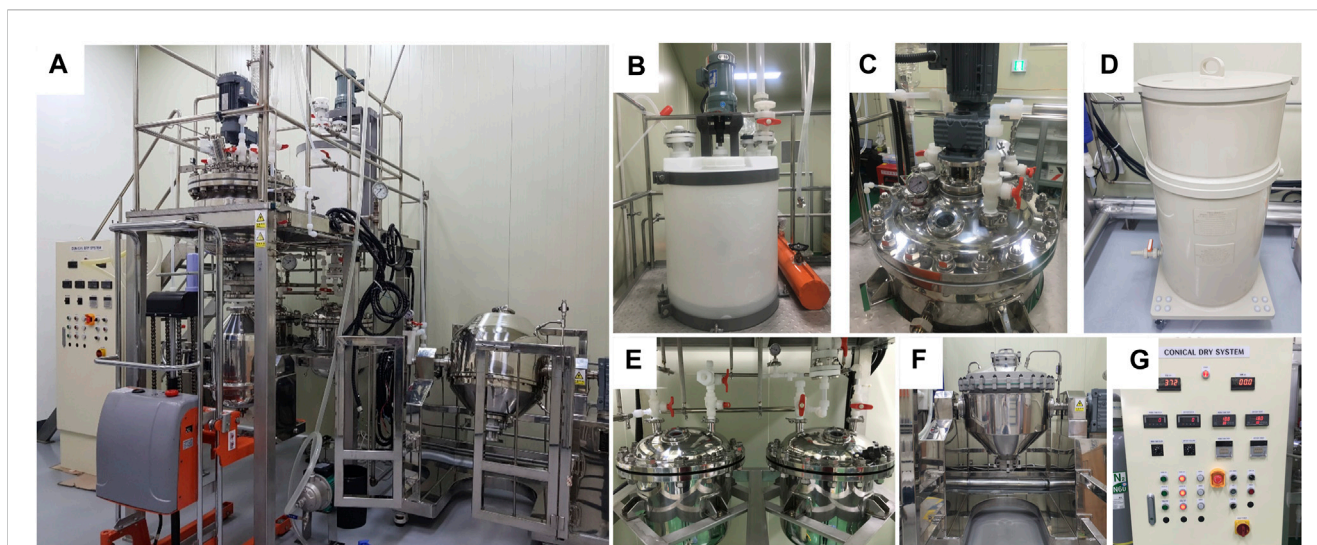


**FIGURE 1**

(A) Mass purification facility, (B) Feed tank for dissolving the NaI, (C) Mixing tank for boiling solution and recrystallization process, (D) Filter unit for separation of NaI crystal and mother liquor, (E) Receiver tanks for collecting vapor from mixing tank and dryer, (F) Conical dryer for the NaI powder drying, (G) Main controller to control all the equipment.

and reach a definitive conclusion of the DAMA/LIBRA experiment results, we are preparing the COSINE-200 experiment as the next phase of the COSINE-100 [17, 28]. The main goal of the COSINE-200 is to develop 200 kg of ultra-low background NaI(Tl) crystals with a background level lower than those of the DAMA/LIBRA. To reach the physics goal of COSINE-200, we have been developing technology for the low-background NaI(Tl) detector that includes the mass production of ultra-low background NaI powder, crystal growing techniques, and detector assembly [17, 28, 29]. The first step is preparing the ultra-low background NaI powder, in which the potassium concentration must be below 20 ppb and the lead concentration less than 1 ppb. An activity level of  $^{210}\text{Pb}$  was as low as 0.01 mBq/kg in NaI(Tl) crystal grown with NaI powder containing 1 ppb of lead [17]. Radioactivity-wise, commercially available Astro-grade NaI powders from Sigma-Aldrich are suitable for ultra-low background NaI(Tl) crystal synthesis [17, 30]. Still, their extremely high-cost demands independent development of mass purification technology. We have investigated a recrystallization technique to purify the NaI powder at a reasonable price [31]. The lab-scale procedure provided a satisfactory performance of the potassium and lead reduction. Based on successful lab-scale experiments, the mass purification facility was established at the Institute for Basic Science (IBS) in Daejeon, Korea [29]. For the last 2 years, we optimized operational parameters for the mass production of ultra-low background NaI powder. The yield efficiencies for the chemical process were balanced *versus* the products' purity. The processing conditions were adapted to recycle the mother solution and recover NaI from the melt residual after the crystal growth. Using developed technology, we have produced about 480 kg of the low-background powder with a production capability of 35 kg per 2 weeks. Using the purified NaI powder, the radioactive background was reduced at least twice in a small size of NaI(Tl) crystal relative to the COSINE-100 crystals [32]. This report summarizes our experience, describes the mass purification facility, optimized raw

powder purification, and the recovery of NaI from the mother solution and residual melt.

## 2 Materials and methods

We use NaI powder from Merck (99.99 (5)% purity, Optipure<sup>®</sup>) as an initial material. The potassium contamination in the specially ordered powder is below 1 ppm. High resistance, 18.2 M $\Omega$  cm de-ionized (DI) water is a solvent to dissolve the NaI powder. We use absolute ethanol (~200 proof, HPLC grade, ACS) from Scharlau to wash the recrystallized NaI crystals. Hydrophilic PTFE membrane filters with 1.0  $\mu\text{m}$  pore size from Advantec are used to separate the recrystallized NaI crystals from the mother liquor.

The mass production facility of the ultra-low background NaI powder is shown in Figure 1A. It consists of two main reactors (Figures 1B,C), a Nutsche filter unit (Figure 1D), two receivers (Figure 1E), and a conical dryer (Figure 1F). The operation of the whole system, including temperature control through the oil circulation system, is performed by the main controller in Figure 1G. The feed tank (Figure 1B) is used for powder dissolution and pre-processing to prevent oxidation of the iodide ions. Two main reactors in Figures 1B,C are connected, utilizing the polypropylene (PP) pipes that transfer the NaI solution from the feed tank to the mixing tank (Figure 1C), as shown in Figure 1A. A cartridge filter is installed in the middle of the PP pipelines to remove the insoluble impurities from the solution. The mixing tank performs the recrystallization using the temperature dependence of the NaI solubility in the water [33]. We evaporate water from the NaI solution until it becomes oversaturated at 110  $^{\circ}\text{C}$  (Figure 2A), then cool the mixing tank down to 30  $^{\circ}\text{C}$  while stirring the solution (Figure 2B). In this process, pure NaI crystals grow without agglomeration, while soluble impurities remain in the mother solution. The crystals are separated from the mother solution by the PTFE membrane filter (Figure 2C). The crystals are washed with

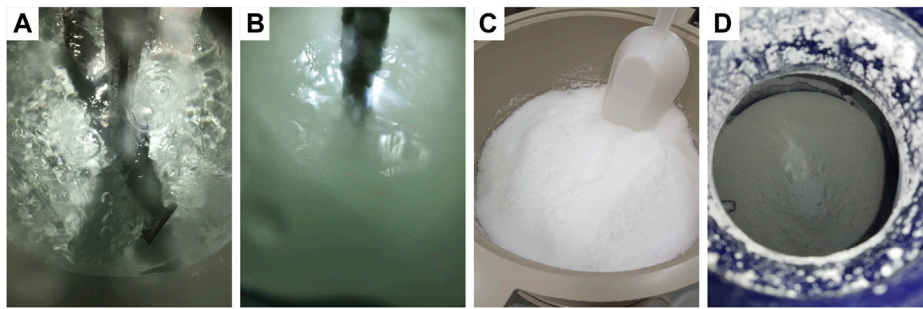


FIGURE 2

(A) Boiling of solution with stirring, (B) Recrystallized NaI crystal with mother liquor, (C) Filtrated and washed NaI crystal on the filter unit, (D) Dried NaI powder in the conical dryer.

**TABLE 1** Representative ICP-MS results of raw and purified powders vs. Astro-grade powder's purity. Uncertainties are given at 90% C.L., and upper limits are given at 95% C.L.

Description	K	Fe	Sr	Ba	Pb	Th	U
	ppb	ppb	ppb	ppb	ppb	ppt	ppt
Astro grade	5 ± 3	110 ± 20	0.3 ± 0.1	0.6 ± 0.1	0.8 ± 0.5	<6	<6
Merck-raw powder	250 ± 90	33 ± 6	19 ± 1	3.0 ± 0.4	40 ± 2	<6	<6
Purified powder (20–5)	11 ± 1	<10	0.3 ± 0.1	0.9 ± 0.1	0.5 ± 0.1	<6	<6
Mother solution (20–5)	550 ± 120	<200	38 ± 2	9 ± 1	60 ± 4	<6	<6

**TABLE 2** Representative HPGe result of purified powder from raw powder purification. The upper limits are given at 90% C.L.

$^{226}\text{Ra}$ ( $^{238}\text{U}$ )	$^{40}\text{K}$	$^{228}\text{Ac}$	$^{228}\text{Th}$
<0.56 mBq/kg	<5.64 mBq/kg	<1.10 mBq/kg	<0.71 mBq/kg

chilled ethanol to rinse off the remaining mother liquor and impurities from the crystal surface. The washed crystals are dried in the conical dryer (Figure 2D). The produced powders are packed in HDPE bottles and stored in the desiccators to avoid moisture absorption. The details of the facility and recrystallization procedure are described elsewhere in [29].

Radiopurity in the raw and purified powders and the mother solution from the purification process is measured by an inductively coupled plasma mass spectrometry (ICP-MS) and high-purity Germanium (HPGe) detector [34]. The water content in the produced powders is measured by the Karl-Fisher titrator. The purity and moisture content of the final product are always checked batch by batch.

## 3 Results

### 3.1 Raw powder purification

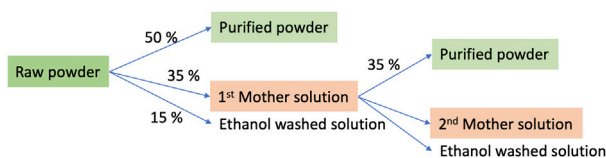
The main goal of our purification is to reduce internal potassium (K) contamination to less than 20 ppb. Table 1 and

Tables 2 show the representative measurements from the raw powder purification process by ICS-MS and HPGe, respectively. As shown in Table 1, most of the potassium contamination from the raw powder was filtrated and concentrated in the mother solution. Potassium and lead concentrations in the purified powders were reduced by 20 and 80 times, resulting in final amounts of 11 ppb and 0.5 ppb, respectively. Significant reduction of Sr and Ba below the ppb level may indicate a reduction of radium, which belongs to the same family group of the periodic table. With a single crystallization procedure with about 40% yield efficiency, the purity of the produced powder became similar to the Astro-grade powder. The impurity concentrations in the mother solutions were increased approximately twice as in the raw powder. Twenty days of HPGe counting using 1.2 kg of purified powder sampled in the Marinelli beaker reported only upper limits for  $^{226}\text{Ra}$ ,  $^{228}\text{Ac}$ ,  $^{228}\text{Th}$ , and  $^{40}\text{K}$ , as seen in Table 2.

To improve production capacity while maintaining the high quality of the product, we continually performed the raw powder purification with slightly different initial charges and recovery yields, as summarized in Table 3. Although the powder charge was increased from 40 kg to 64 kg, the purified product had similar purities from batch to batch. However, a high recovery yield of 58% provided considerable contamination of K, about 38 ppb. In case of the recovery yields were less than 50%, the purified powder contained consistently low contamination, especially K, about 10 ppb. To keep the consistent and high quality of the product, we ascertained a

**TABLE 3** The ICP-MS results of purified powders in different batches of raw powder purification. Uncertainties are given at 90% C.L, and upper limits are given at 95% C.L.

Sample no.	Initial charge	Recovery yield	K ppb	Fe ppb	Sr ppb	Ba ppb	Pb ppb	Th ppt	U ppt
20-5	40 kg	44%	11 ± 1	<10	0.3 ± 0.1	0.9 ± 0.1	0.5 ± 0.1	<6	<5
20-7	50 kg	41%	10 ± 1	<10	0.1 ± 0.1	0.3 ± 0.1	<0.3	<3	<5
20-8	50 kg	39%	6.4 ± 0.1	<10	0.1 ± 0.1	0.7 ± 0.1	<0.3	<3	<5
21-5	53 kg	42%	5.4 ± 0.3	<10	0.2 ± 0.1	0.4 ± 0.1	0.5 ± 0.1	<5	<3
21-8	60 kg	58%	38 ± 2	<10	0.4 ± 0.1	0.3 ± 0.1	0.5 ± 0.1	<7	<7
22-5	64 kg	35%	11 ± 1	<7	0.4 ± 0.1	1.6 ± 0.2	0.9 ± 0.5	<100	<20
The overall range of impurities within 35%–44% recovery yield (min/max)			5.1/12	<7/<10	0.1/0.5	0.2/1.8	<0.3/1.4	<3/<100	<3/<20

**FIGURE 3**  
Material balances in the NaI recovery cycle.

50% yield efficiency at maximum for our purification process. Routine purification works have made our experience proficient for the last 2 years. Compared to the initial investigation shown in Ref. [29], we obtained consistently stable products with the required background level using the same purification facility. With the above-optimized purification parameters, the process took 2 weeks. Recrystallizing the raw powder took about three working days with 70 kg of the initial charge, and another seven working days were required to dry the wet crystals. With 40–50% recovery efficiency, 30–35 kg of purified powder could be produced in a cycle.

### 3.2 Mother solution recovery

After the purification process, the mother solution is the remaining product with concentrated impurities from the initial material. In the optimized purification process, 50% of the initial charge was collected as the purified dry product. Another 35% of NaI remained in the mother solution, and 15% was washed out with ethanol, as shown in Figure 3. In three cycles of the raw powder purification, the amount of NaI collected as the mother solution was enough for further recycling. We recovered this mother solution in the same manner but reduced the target recovery efficiency from 50% to 35% due to the relatively high impurity level in the mother solution. As summarized in Table 4, the recovered crystals from the mother solution contained higher impurities than those obtained from the raw powder purification. The K contaminations varied from 18 to <50 ppb, proportional to the initial impurities in the mother solution. When the K content in the initial mother solution was higher

than 1,000 ppb, reaching 20 ppb of K was challenging with a single treatment. In this case, an additional recrystallization cycle of the powder was necessary to reach our goal of purity. However, the following recrystallization of the crystals recovered from the first mother solution (MS-1) was inefficient in production rate. Thus, the rational K level in the initial solution must be lower than 1 ppm.

As shown in Figure 3, after the separation of crystals from the MS-1, the second mother solution (MS-2) contained about 50% NaI and accumulated most impurities. The MS-2 mostly had K content over 1 ppm. Double recrystallization would be unavoidable to recover this NaI remained. We did not consider recycling the MS-2 due to low recovery efficiency compared to the workforce required.

### 3.3 Residual melt recovery

We designed a large-size Kyropoulos grower to synthesize 120 kg NaI(Tl) crystal ingot [17]. In this grower, about 200 kg of NaI powder was loaded and melted in the quartz crucible. Crystal-growing trials using Merck raw powders were performed a couple of times with partial success. After pulling out the crystal ingot, many residues remained in the quartz crucible. Typical impurities in the residual melt after growing were approximately twice as high as that in the loaded powder due to the segregation effect. Nevertheless, the recovery of the residual melts was successfully made by achieving satisfactory purity levels, as summarized in Table 5. The K concentration in the produced powders varied from 8 to 11 ppb. The purity of recovered NaI from the melt is expected to be much purer if we use the purified powder for mass crystal growth.



**TABLE 4** The ICP-MS result of the mother solution recovery experiment in different batches of mass production. It is marked as (M) for the naming. In this experiment, the initial solution means the initial mother solution and the Wet crystal means recrystallized and washed crystal. If the purity is not accepted, then additional recrystallization is required, so the purity was confirmed first by ICP-MS before drying and then dried thoroughly. The wet crystal consists of 73% ± 2% NaI and extra water and ethanol, so the impurity concentration is calculated as 73% NaI. Uncertainties are given at 90% C.L, and upper limits are given at 95% C.L.

Sample no.	Material	Approx. recovery yield	K ppb	Fe ppb	Sr ppb	Ba ppb	Pb ppb	Th ppt	U ppt
21-7(M)	Initial sol		470 ± 10	N/A	34 ± 1	7.3 ± 0.2	56 ± 1	<7	<7
	Wet cryst	~55%	<50	N/A	1.2 ± 0.1	0.2 ± 0.1	2.0 ± 0.1	<7	<7
21-11(M)	Initial sol		610 ± 30	16 ± 1	40 ± 2	10 ± 1	88 ± 12	<7	<7
	Wet cryst	~55%	18 ± 1	<7	1.0 ± 0.1	0.2 ± 0.1	4.5 ± 0.3	<7	<7
22-2(M)	Initial sol		1,010 ± 150	8 ± 1	16 ± 1	15 ± 1	86 ± 4	<4	<4
	Dry powder	~45%	21 ± 2	<7	0.2 ± 0.1	0.7 ± 0.1	1.0 ± 0.1	<4	<4
20-3(M)	Initial sol		1,170 ± 120	39 ± 2	33 ± 2	12 ± 1	60 ± 2	<6	<5
	Dry powder	~35%	44 ± 5	14 ± 1	1.0 ± 0.1	0.4 ± 0.1	2.0 ± 0.1	<6	<5
21-4(M)	Initial sol		330 ± 40	N/A	20 ± 1	6.3 ± 0.2	41 ± 4	<5	<3
	Wet cryst	~35%	<40	N/A	0.4 ± 0.1	0.1 ± 0.1	1.2 ± 0.1	<5	<3

**TABLE 5** The ICP-MS result of residual melt recovery experiment in different batches of mass production. It is marked as (RM) for the naming, and the Initial solution is the residual melt solution after dissolving melt and filtration of the quartz particles. The Wet crystal samples were taken after recrystallization and washing with ethanol. Uncertainties are given at 90% C.L, and upper limits are given at 95% C.L.

Sample no.	Material	Recovery yield	K ppb	Fe ppb	Sr ppb	Ba ppb	Pb ppb	Th ppt	U ppt
21-12 (RM)	Initial sol		730 ± 10	20 ± 2	10 ± 1	8.0 ± 0.6	143 ± 12	<7	<7
	Wet cryst	53%	8 ± 1	<10	0.4 ± 0.1	0.3 ± 0.1	5 ± 1	<7	<7
21-13 (RM)	Initial sol		540 ± 20	N/A	10 ± 1	5.1 ± 0.2	95 ± 10	<7	<7
	Wet cryst	40%	<50	N/A	0.1 ± 0.1	<0.1	<0.3	<7	<7
22-1 (RM)	Initial sol		390 ± 10	N/A	8 ± 1	6.4 ± 0.2	40 ± 4	<4	<4
	Dry powder	44%	8 ± 1	<7	0.1 ± 0.1	0.3 ± 0.1	0.7 ± 0.1	<4	<4
22-4 (RM)	Initial sol		570 ± 10	N/A	15 ± 2	6.7 ± 0.5	5 ± 1	<4	<4
	Dry powder	48%	11 ± 4	<7	0.1 ± 0.1	0.3 ± 0.1	<0.3	<4	<4

The process of recovering NaI from the collected residual melt differed from the original purification method because the melt contained a significant amount of insoluble quartz particles and dust. Before the usual operation, the NaI melt dissolved in water was filtered with the PTFE membrane filter. Considering the evaporation of iodine during the crystal-growing process, a three times higher dose of hydrogen iodide (HI) was introduced to reach pH 3.5. All other processes of recrystallization and target recovery efficiency were the same as raw powder purification.

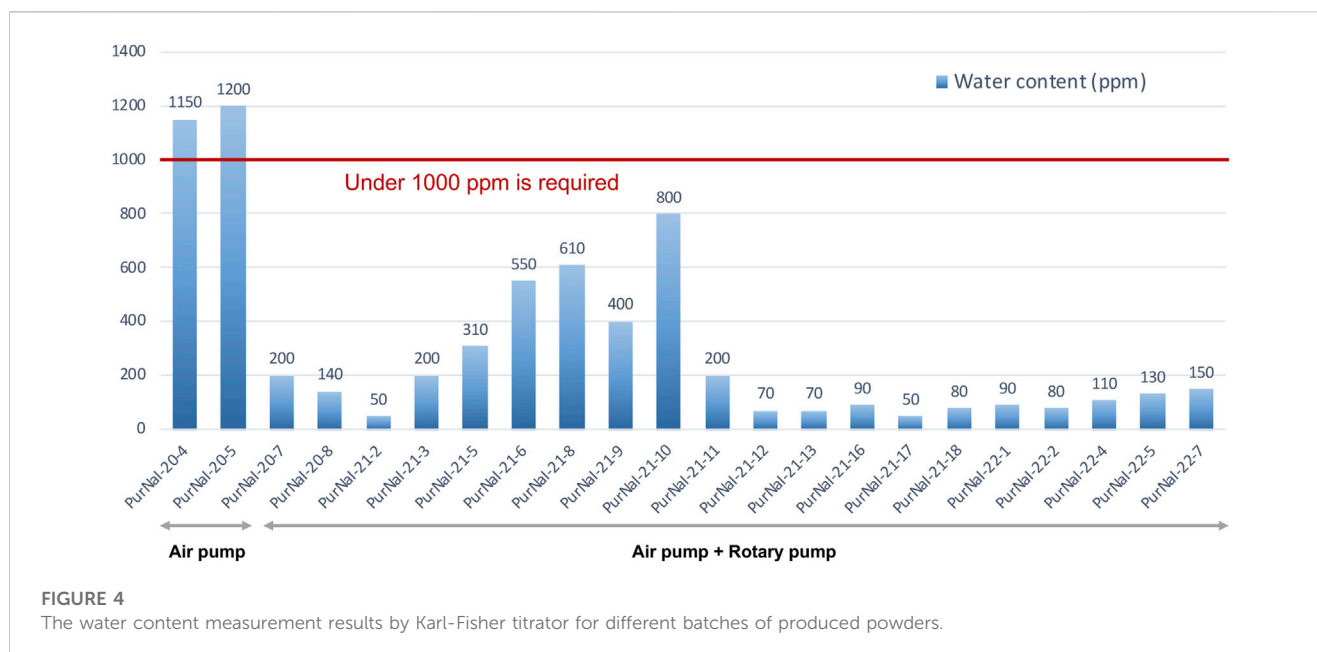
### 3.4 Water content measurement

Sodium iodide is highly hygroscopic, and its chemical interaction with moisture produces NaOH when heated and causes corrosion of the quartz crucible used in the growing crystal [35]. Keeping the water content below 1,000 ppm in the produced powder was crucial. All recrystallized powders were dried in two-step processes. In the first

step, the wet powder was dried at 65 °C to avoid agglomerating the NaI powders with water inside the dryer. Then the temperature was increased to 130 °C to dry the powder completely. The vapor released from the drying process was extracted with a vacuum pump. Initially, we used a chemical resistance air pump with relatively low pressure to protect the pump from corrosive vapor. As seen in Figure 4, reaching moisture content below 1,000 ppm in the dried powders with the previous set-up was impossible. We improved our drying system by introducing a high-pressure rotary pump with traps for corrosive vapor during the high-temperature drying process. We achieved the water content to less than 1,000 ppm with modified set-up.

## 4 Discussion

A facility for mass production of the ultra-pure NaI powder for the COSINE-200 experiment operates well with extensive parameter optimization. The purification of raw NaI powder, the recycling of



the mother solution, and the recovery of NaI from the residual melt were performed in parallel. We have produced about 480 kg of low-background powder with a successful reduction of the internal contamination that is pure enough for the COSINE-200 detectors. The optimized parameters with a stable operation process have provided a maximum 35 kg powder production capacity in 2 weeks, but there is still room for improvement. If we increase the volume of the dryer twice, then two recrystallization cycles can be performed in a week in the same manner and dried together in the bigger dryer. The production capacity will be increased up to 70 kg in 2 weeks while keeping the powder quality. With improved capacity, successive double crystallization can help to reach a potassium level much lower than 5 ppb using the above-described facility. We can smoothly provide the ultra-low background NaI powder for the mass production of the NaI(Tl) crystals for the COSINE-200 experiment.

## Data availability statement

The raw data supporting the conclusions of this article will be made available by the authors, without undue reservation.

## Author contributions

KS, OG, AI, and HL contributed to the conception, original design and technical performance of the study. KS, CL and YK

performed routine purification. JC performed the ICP-MS analysis. EL contributed to the HPGe array measurement performance. KS wrote the first draft of the manuscript. All authors contributed to manuscript revision, read, and approved the submitted version.

## Funding

This work is supported by the Institute for Basic Science (IBS) under project code IBS-R016-A1.

## Conflict of interest

The authors declare that the research was conducted in the absence of any commercial or financial relationships that could be construed as a potential conflict of interest.

## Publisher's note

All claims expressed in this article are solely those of the authors and do not necessarily represent those of their affiliated organizations, or those of the publisher, the editors and the reviewers. Any product that may be evaluated in this article, or claim that may be made by its manufacturer, is not guaranteed or endorsed by the publisher.

## References

1. Clowe D, Bradač M, Gonzalez AH, Markevitch M, Randall SW, Jones C, et al. A direct empirical proof of the existence of dark matter. *Astrophys J* (2006) 648:L109–13. doi:10.1086/508162
2. Baudis L. Dark matter detection. *J Phys G: Nucl Part Phys* (2016) 43:044001. doi:10.1088/0954-3899/43/4/044001
3. Bertone G, Hooper D. History of dark matter. *Rev Mod Phys* (2018) 90:045002. doi:10.1103/revmodphys.90.045002
4. Arcadi G, Dutra M, Ghosh P, Lindner M, Mambrini Y, Pierre M, et al. The waning of the wimp? A review of models, searches, and constraints. *Eur Phys J C* (2018) 78:203. doi:10.1140/epjc/s10052-018-5662-y

5. Aghanim N, Akrami Y, Ashdown M, Aumont J, Baccigalupi C, Ballardini M, et al. Planck 2018 results. VI. Cosmological parameters. *Astron Astrophys* (2020) 641:A6. doi:10.1051/0004-6361/201833910
6. Adhikari G, Adhikari P, de Souza EB, Carlin N, Choi S, Djamal M, et al. An experiment to search for dark-matter interactions using sodium iodide detectors. *Nature* (2018) 564:83–6. doi:10.1038/s41586-018-0739-1
7. Adhikari G, Carlin N, Choi J, Choi S, Ezeribe A, Franca L, et al. Searching for lowmass dark matter via the Migdal effect in COSINE-100. *Phys Rev D* (2022) 105:042006. doi:10.1103/PhysRevD.105.042006
8. Bernabei R, Belli P, Bussolotti A, Cappella F, Caracciolo V, Cerulli R, et al. First model independent results from DAMA/LIBRA–Phase2. *Universe* (2018) 4:116. doi:10.3390/universe4110116
9. Zani A, D'Angelo D, Vignoli C, Di Carlo G, Di Giacinto A, Ianni A, et al. The SABRE experiment. *Int J Mod Phys A* (2022) 37:2240016. doi:10.1142/S0217751X22400164
10. Adhikari G, Carlin N, Choi J, Choi S, Ezeribe A, Franca L, et al. Searching for lowmass dark matter via the Migdal effect in COSINE-100. *Phys Rev D* (2022) 105:042006. doi:10.1103/PhysRevD.105.042006
11. Aprile E, Aalbers J, Agostini F, Alfonsi M, Althueser L, Amaro D, et al. Dark matter search results from a one ton-year exposure of xenon1t. *Phys Rev Lett* (2018) 121:111302. doi:10.1103/PhysRevLett.121.111302
12. Amole C, Ardid M, Arnquist IJ, Asner DM, Baxter D, Behnke E. Dark matter search results from the complete exposure of the PICO-60 C<sub>3</sub>F<sub>8</sub> bubble chamber. *Phys Rev D* (2019) 100:022001. doi:10.1103/PhysRevD.100.022001
13. Fushimi K, Kanemitsu Y, Hirata S, Chernyak D, Hazama R, Ikeda H, et al. Development of highly radiopure NaI(Tl) scintillator for PICOLON dark matter search project. *Prog Theor Exp Phys* (2021) 2021:043F01. doi:10.1093/ptep/ptab020
14. Bernabei R, Belli P, Cappella F, Caracciolo V, Castellano S, Cerulli R, et al. Final model independent result of DAMA/LIBRA–phase1. *Eur Phys J C* (2013) 73:2648. doi:10.1140/epjc/s10052-013-2648-7
15. Bernabei R, Belli P, Bussolotti A, Cappella F, Caracciolo V, Cerulli R, et al. The DAMA project: Achievements, implications and perspectives. *Prog Part Nuc Phys* (2020) 114:103810. doi:10.1016/j.pnpnp.2020.103810
16. Savage C, Gelmini G, Gondolo P, Freese K. Compatibility of DAMA/LIBRA dark matter detection with other searches *J Cosmol Astropart Phys* 2009, 010 (2009). doi:10.1088/1475-7516/2009/04/010
17. Park BJ, Choi J, Choe J, Gileva O, Ha C, Iltis A, et al. Development of ultra-pure NaI(Tl) detectors for the COSINE-200 experiment. *Eur Phys J C* (2020) 80:814. doi:10.1140/epjc/s10052-020-8386-8
18. Bernabei R, Belli P, Cappella F, Caracciolo V, Cerulli R, Dai CJ, et al. No role for neutrons, muons and solar neutrinos in the DAMA annual modulation results. *Eur Phys J C* (2014) 74:3196. doi:10.1140/epjc/s10052-014-3196-5
19. Adhikari G, Carlin N, Choi J, Choi S, Ezeribe A, França L. An induced annual modulation signature in COSINE-100 data by DAMA/LIBRA's analysis method. *Sci.Rep.* (2023) 13:4676. doi:10.1038/s41598-023-31688-4
20. Adhikari G, de Souza EB, Carlin N, Choi JJ, Choi S, Djamal M, et al. Strong constraints from COSINE-100 on the DAMA dark matter results using the same sodium iodide target. *Sci Adv* (2021) 7:eabk2699. doi:10.1126/sciadv.abk2699
21. Adhikari G, de Souza EB, Carlin N, Choi JJ, Choi S, Djamal M, et al. Background modeling for dark matter search with 1.7 years of COSINE-100 data. *Eur Phys J C* (2021) 81:837. doi:10.1140/epjc/s10052-021-09564-0
22. Prihadi H, Adhikari G, De Souza EB, Carlin N, Choi J, Choi S, et al. Measurement of the cosmic muon annual and diurnal flux variation with the COSINE-100 detector. *J Cosmol Astropart Phys* (2021) 2021:013. doi:10.1088/1475-7516/2021/02/013
23. Kim H, Adhikari G, Barbosa de Souza E, Carlin N, Choi J, Choi S, et al. The environmental monitoring system at the COSINE-100 experiment. *J Instrum* (2022) 17:T01001. doi:10.1088/1748-0221/17/01/t01001
24. Ko YJ, Adhikari G, Adhikari P, de Souza EB, Carlin N, Choi J. Comparison between DAMA/LIBRA and COSINE-100 in the light of quenching factors. *J Cosmol Astropart Phys* (2019) 1911:008. doi:10.1088/1475-7516/2019/11/008
25. Adhikari G, Adhikari P, de Souza EB, Carlin N, Choi S, Djamal M, et al. Search for a dark matter-induced annual modulation signal in NaI(Tl) with the COSINE-100 experiment. *Phys Rev Lett* (2019) 123:031302. doi:10.1103/PhysRevLett.123.031302
26. Adhikari G, de Souza EB, Carlin N, Choi J, Choi S, Ezeribe A, et al. Three-year annual modulation search with COSINE-100. *Phys Rev D* (2022) 106:052005.
27. Adhikari P, Carlin N, Choi J, Choi S, Ezeribe A, Franca L. Background model for the NaI(Tl) crystals in COSINE-100. *Eur Phys J C* (2018) 78:490. doi:10.1140/epjc/s10052-018-5970-2
28. Choi J, Park B, Ha C, Kim K, Kim S, Kim Y, et al. Improving the light collection using a new NaI(Tl) crystal encapsulation. *Nucl Instrum Methods Phys Res A* (2020) 981:164556. doi:10.1016/j.nima.2020.164556
29. Shin K, Choe J, Gileva O, Iltis A, Kim Y, Lee C, et al. A facility for mass production of ultra-pure NaI powder for the COSINE-200 experiment. *J Instrum* (2020) 15:C07031. doi:10.1088/1748-0221/15/07/c07031
30. Shields E, Xu J, Calaprice F. Sabre: A new NaI(Tl) dark matter direct detection experiment. *Phys Proce* (2015) 61:169–78. doi:10.1016/j.phpro.2014.12.028
31. Shin K, Gileva O, Kim Y, Lee HS, Park H. Reduction of the radioactivity in sodium iodide (NaI) powder by recrystallization method. *J Rad Nuc Chem* (2018) 317:1329–32. doi:10.1007/s10967-018-6006-y
32. Lee H, Park B, Choi J, Gileva O, Ha C, Iltis A, et al. Performance of an ultra-pure NaI(Tl) detector produced by an indigenously-developed purification method and crystal growth for the COSINE-200 experiment. *Front Phys* (2023) 11:1142765. doi:10.3389/fphy.2023.1142765
33. Seidell A. *Solubilities of inorganic and metal organic compounds*. Van Nostrand (1940).
34. Lee MH. Radioassay and purification for experiments at Y2L and yemilab in Korea. *J Phys Conf Ser* (2020) 1468:012249. doi:10.1088/1742-6596/1468/1/012249
35. Suerfu B, Calaprice F, Souza M. Zone refining of ultrahigh-purity sodium iodide for low-background detectors. *Phys Rev* (2021) 16:014060. doi:10.1103/physrevapplied.16.014060